Machine learning-based diagnosis of eye-diseases

Thanaa Hasan Yousif, Nahla Ali Tomah, Marwa Jaleel Mohsin
Engineering Technical College, Al-Furat Al-Awsat Technical University, Al-Najaf, Iraq

Article Info

Article history:

Received Nov 15, 2022
Revised Aug 5, 2023
Accepted Aug 15, 2023

Keywords:

Artificial intelligence
Artificial neural networks
Choroidal neovascularization
Diabetic macular edema
Eyes disease prediction
Machine learning

ABSTRACT

Over the last several years, artificial intelligence (AI) has been substantially utilized in image processing and classification. Several tools are accessible for visualizing, training, and pre-processing image data. One such tool is orange, which has several pre-processing modules and a particular add-on for image processing methods in addition to excellent data visualization. The tool (version 3.32.0) was used in the suggested study to give a comparative and predictive analysis using several classification models. Three main models have been used to train and predict the three groups image eye diseases. The results were compared based on some criteria, including area-under-a-curve (AUC), the accuracy of classification (CA), F1 score, precision, and recall. These models include K-nearest neighbour (KNN), logistic regression (LR), artificial neural networks (ANN) and stacking model. The stacking model, which is a novel model, is also presented in this work by concatenating the output of the parallel form of ANN and KNN models with the LR model. The best performance belonged to the Stacking model, which offers the best detection and prediction results.

Corresponding Author:

Marwa Jaleel Mohsin
Engineering Technical College, Al-Furat Al-Awsat Technical University
Al-Najaf, Iraq
E-mail: marwa.jaleel@atu.edu.iq

1. INTRODUCTION

The classification of images has emerged as a leading research image in a variety of fields. Optical wireless communication (OWC) is an the classification of images has emerged as a leading research image in a variety of fields, including data mining [1], computer vision, and medical image analysis However, most photographs are unstructured data that must be converted into a structured format before being processed effectively [2]. Therefore, it is helpful to extract significant characteristics of the photos that various artificial intelligence (AI) approaches may be employed for classification of the image [2]. Also, more billion of photographs accessible on the internet could be readily gathered, and various data mining software may be utilized to apply AI approaches for categorizing the images appropriately [3].

The subfields of AI such as deep learning and machine learning require extracting features from data and then using those characteristics to grasp the data's precise form and qualities [4], [5]. Furthermore, deep learning approaches mine the characteristics automatically and utilize them to analyze the images [6], [7]. Multiple models are available for the classification of images; thus, it is required to justify which model is most appropriate for image classification. Furthermore, numerous platforms, such as programming languages or tools, may be utilized to implement these methods. Orange data mining is a free tool that can be used to pre-process data, see how it looks, and put various classification and clustering patterns into action. Also, orange has option to add extra models for applications like bio-informatics, network-analyses, and image-analyses [6]. This study used various AI algorithms to classify the images and measure their effectiveness based on including area-under-a-curve (AUC), the accuracy of classification (CA), F1 score, accuracy, and recall. The pattern assessment was carried out using orange data mining, and the results were used both as a forecast for another set that had not been trained by any of the models that were used in this study, and as the final result.

2. INPUT DATA FOR TESTING AND TRAINING

The database that can be seen on the Kaggle website was used in this study. Kaggle is a Google company, it's a network of data scientists and engineers working in machine learning. Kaggle is an online hub for the data science community, where members may share and explore data sets, research and build AI models, work together with peers in the field, and compete against one another to solve data science problems [8], [9]. About 6,000 of the total images was utilised for the proposed algorithms to identify two types of eye diseases, and compare them with healthy eye images (normal eyes). Therefore, each class has 2,000 images with a 90% training ratio. We chose two types of eye disease to identify from normal eye images. The image data feeds into the workspace to program as an image using the import images widget. This work dealts with two types of eye diseases:

2.1. Choroidal neovascularization (CNV) disease

About 5% of eyes have CNV, a late manifestation that typically appears between the ages of 20 and 45. It's often linked to a "histo spot" in the macula that has been there for a long time. It may form inside a parapapillary lesion on rare occasions. CNV may take place even when there is no previous lesion present. At first, the CNV may leak fluid and cause metamorphopsia, or blurred vision in the centre, and a scotoma [9].

2.2. Diabetic macular edoema (DME) disease

DME is the most common basis of vision loss linked with diabetic retinopathy (DR) and macular laser. DME often makes it hard for people with non-proliferative diabetic retinopathy (NPDR) to see clearly. It is more common in people with type-2 diabetes mellitus (DM2) than type-1 diabetes mellitus (DM1), which accounts for about 12.9% and 7.86% of cases, respectively. There are many things that can cause DME, but the main cause is the breakdown of the blood-retinal barrier, which makes the Henle's macula layer swell [10]. Figure 1 illustrates the samples of retinal retinal optical coherence tomography (Retinal OCT) with Figure 1(a) CNV disease, Figure 1(b) DME disease, and Figure 1(c) normal image used for image classification.

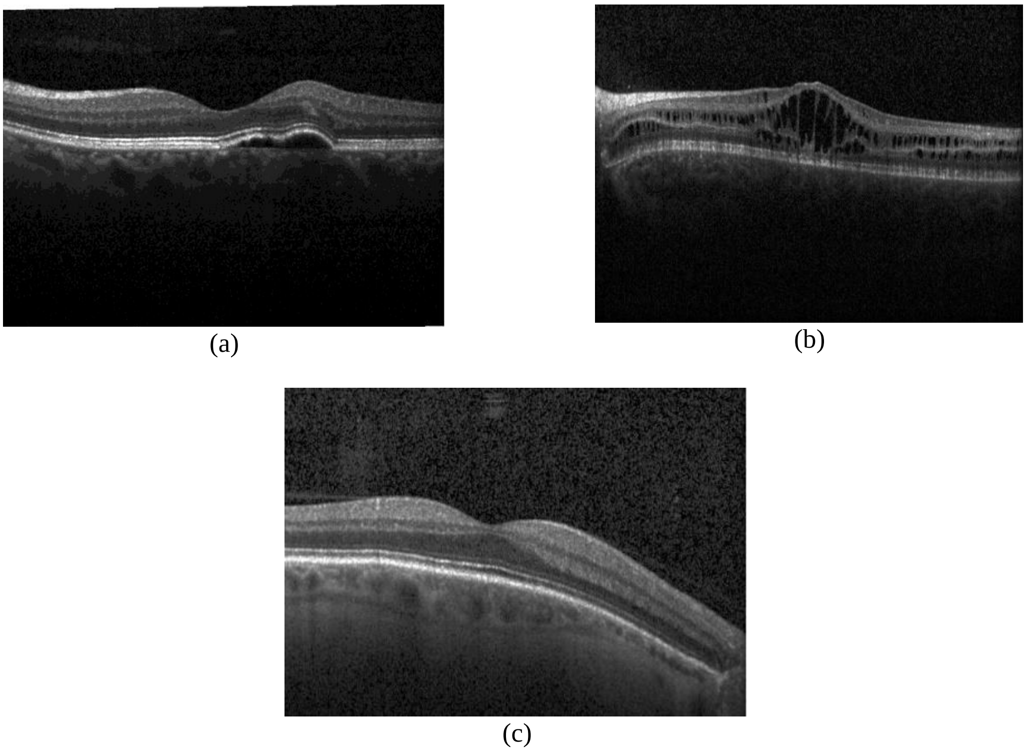

(a) (b)

(c)

Figure 1. The normal and two types of dicease images statuses that used for classification process: (a) CNV disease, (b) DME disease, and (c) normal image

3. IMAGE EMBEDDING

The feature extraction from the photos came after the images had been imported. This step was done by orange's image analysis tool's "image embedding" widget. Subsequently, the photographs were uploaded to the server where feature extraction could take place. Different deep convolutional neural network (DCCN) models were utilized to extract features in this widget. There were several different DCCN models accessible for use in feature mining, including SqueezeNet [11], VGG-16 [12], and inception V3 [13]. Our approach used the SqueezeNet model, which extracted the characteristics locally without transferring the photos to the server. After the procedure, the extracted characteristics were formatted in tables with orange's "data table" widget. SqueezeNet was used to generate meta-features for each image, with a total of 1,000 features assigned to each in addition to the width, height, and size features.

4. IMAGE CLASSIFICATION

The SqueezeNet model was used to extract characteristics from photos, and then three distinct models were used to classify the images based on those features. It was carried out using tenfold cross-validation, in which 80% of the photos were utilized for training and 20% of the images were utilised for testing the models. To begin, each of the models is subjected to training and testing using a variety of parameters. The variables that resulted in the greatest results after checking with various settings are provided, along to an explanation for any model The following sections discuss a variety of trained classifiers [12], [13].

4.1. Artificial neural network (ANN)

ANN is a classification method which uses a mechanism similar to the way in which neurons in the brain function to recognize the underlying link between pictures [14], [15]. Three layers make up a basic of ANN: layer of the input that pick features as input, a layer of the hidden, and layer of the output that decides that category a certain image belongs to [16], [17]. In this work, 100 hidden layers, 100 iterations and the (logistic) function as an activation function were used in this study.

4.2. Logistic regression (LR)

LR utilizes a function of the logistic to create a binary dependent parameter [18]. It is a curve-fitting module in which the dependent value varies in relation to the independent value and the data points are aligned to be as close to the curve as possible [19], [20]. This study, the regularization was carried out with the help of ridge (L2), that reduces the sum of the weight's squares to the greatest extent possible.

4.3. K-nearest neighbour (KNN)

K-closest neighbour, often known as the KNN algorithm, is a basic categorization machine learning approach that has widely applied [21]. Unlabelled tuples are classified using information about their K closest neighbours. K may be assigned the value of any number [22]. The technique requires a target class variable to be used as a label to categories a training dataset after K. Then, KNN determines KNN and designates the most distant class for each unlabelled tuple in the test dataset [23]–[25]. The Euclidean distance was used in this study to construct the index, and the total number of neighbours was eight.

5. PROPOSED ALGORITHMS

Various AI algorithms are utilized to classify the eye images with different satuse of disease and measure their effectiveness based on AUC, CA, F1 score, accuracy, and recall. This work proposed two cases for training and prediction process over three group's image eye diseases; Case 1, Utilised three models, ANN, LR, and KNN, separately for the training and testing process to distinguish the images of two eye diseases, CNV and DME, from the healthy one. Figure 2 illustrate the proposed algorithm for this case, which utilized (6,000) total images (with 2,000 images for each type of eye disease: CNV, DME, and healthy one were chosen for comparison), and the dataset was split into 9:1 ratio for training and testing (The ratio of training 90% with repeat train/test (20), get the highest AC (0.958) for ANN models). For case 2, a new model was presented and we called it the Stacking model. It was a collection of three models: ANN, LR, and KNN. This model combined the ANN and KNN models in a parallel form and then fed the output to the LR model. This scenario exhibits better performance than previouse case in terms of best detection and prediction results. Case 2 for this algorithm is shown in Figure 3 also in the same training is (90%) with repeat train/test (20), get the AC (0.961). Note: this is accurate as an average for three groups of data as the image (CNV, DME, normal).

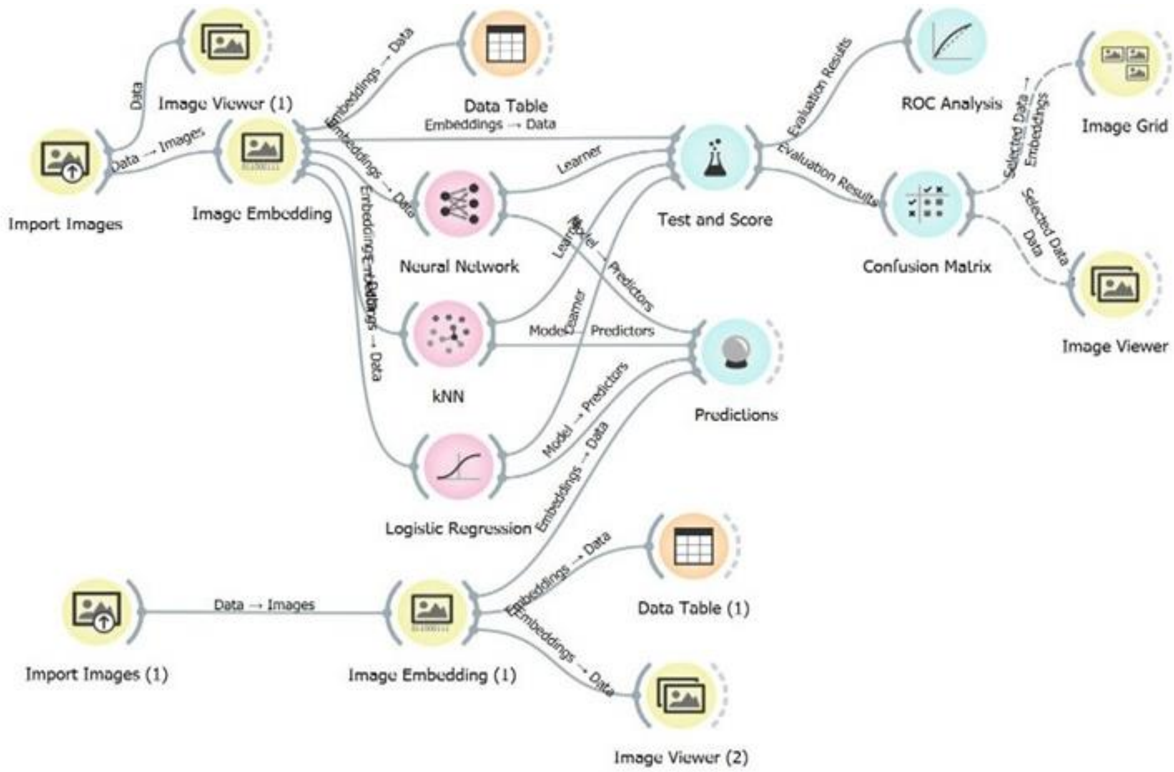

Figure 2. The proposed algorithm of the first case

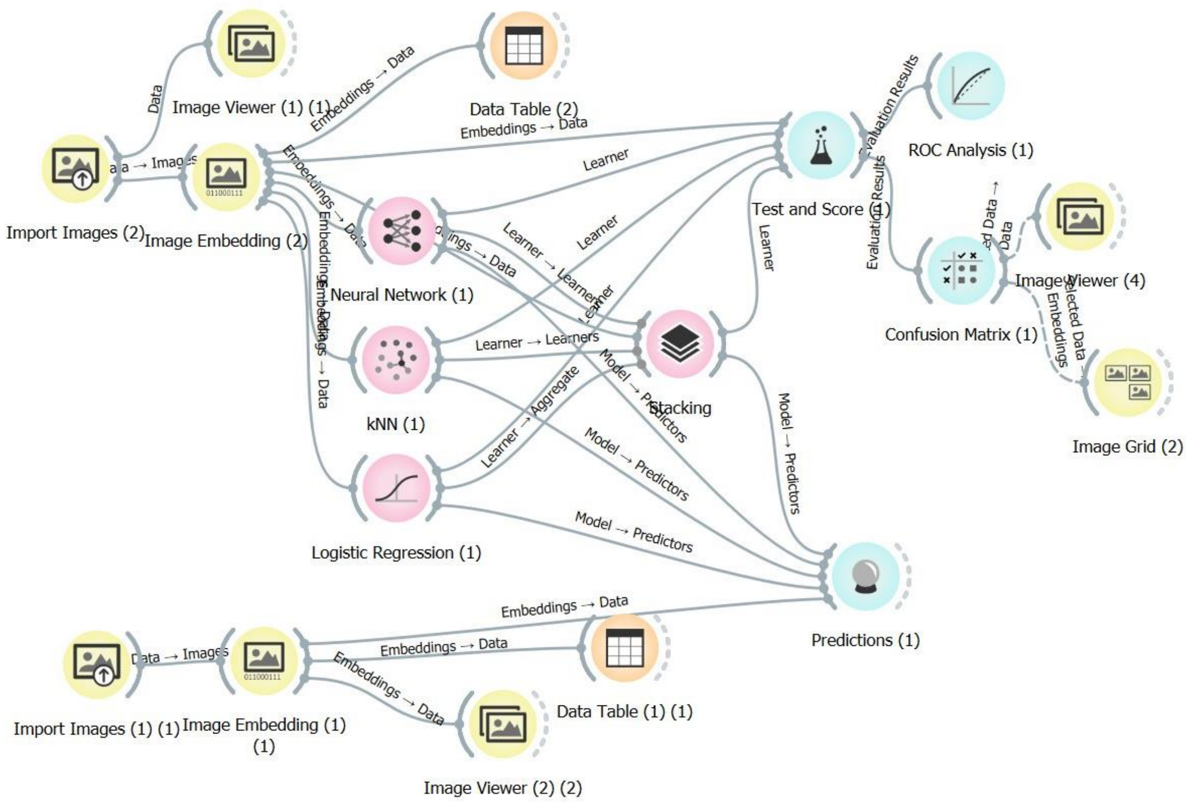

Figure 3. The proposed algorithm of the second case

6. RESULTS AND DISCUSSION

Three different classifiers and prediction procedures were examined to see which performed best. The performance of these models was evaluated based on their CA, precision, recall, F1 score, and AUC values. These indices (these functions) were generated automatically using an orange tool's "test and score" widget. The number of successfully categorized photos was used to quantify the classification accuracy. Precision determined the fraction of positive values that are genuinely positive, whilst recall identified the positive values which were accurately specified. The F1 score was the harmonic mean in terms of precision and recall. The area also showed the quality of the predictions made by trained models under the curve.

Finally, comparisons were made based on the classifiers accuracy, which was an important metric. Figure 4 shows the comparative work, the results of the measuring indices for each diverse classifier were utilized, that the ANN has the highest classification accuracy (0.958). In contrast, LR has an accuracy (0.950) and KNN accuracy (0.901) also in the same training (90%) with repeat training/test (20) for three models. Figure 5 shows the recorded results for the stack model, which exhibits AUC close to ANN with a value (0.994) and better values to CA, F1, precision, and recall (0.961) than each model of a separate case.

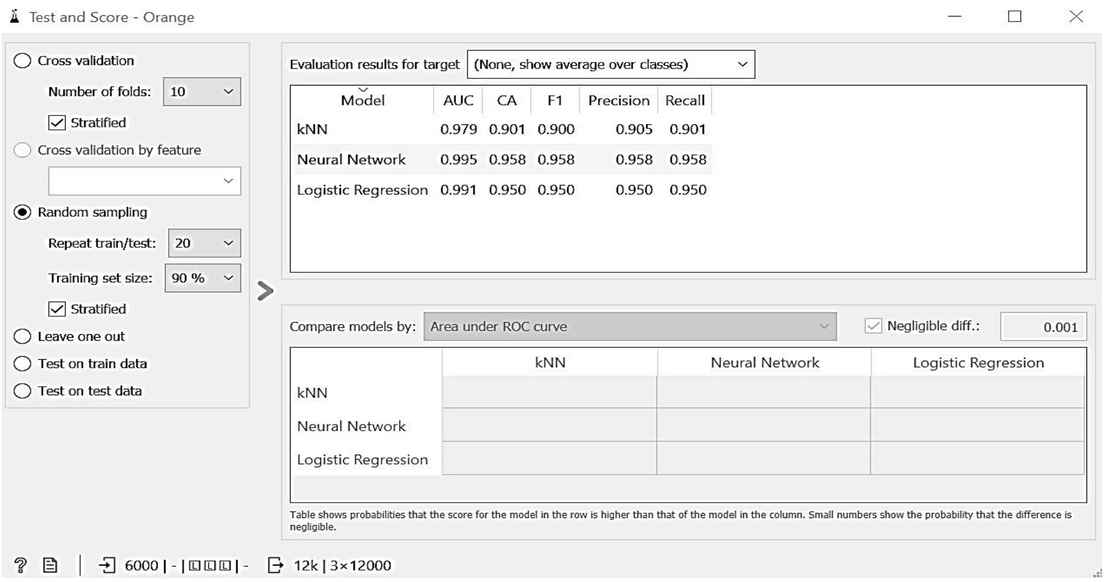

Figure 4. Test and score for case 1

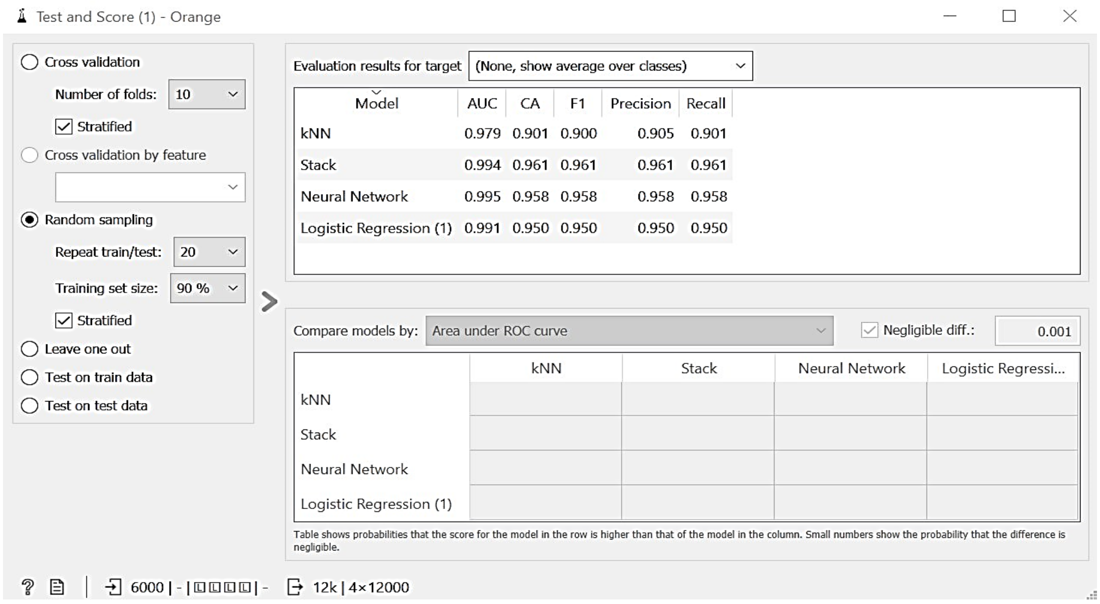

Figure 5. Test and score for case 2

The three alternative classifier models were fed into the "test and score" widget, that outputs the comparison value for each classifier based on CA, precision, recall, F-1 score, and AUC. The "confusion matrix" the widget links with the confusion matrix for each classification model. A confusion matrix can help you determine where the mistake is in a classification process. The diagonal members of the matrix provide the proper classification value, whilst the non-diagonal items provide a mistake when categorizing the photos. The orange tool's "confusion matrix" widget created the confusion matrix for each classifier. The confusion matrix for all of the classification models utilized to classify the images is shown in Figures 6-9.

Confusion Matrix

Confusion matrix for Neural Network (showing number of instances)

		Predicted CNV	DME	NORMAL	Σ
Actual	CNV	3916	66	18	4000
	DME	83	3749	168	4000
	NORMAL	18	152	3830	4000
	Σ	4017	3967	4016	12000

Confusion Matrix

Confusion matrix for Neural Network (showing proportion of actual)

		Predicted CNV	DME	NORMAL	Σ
Actual	CNV	97.9 %	1.6 %	0.5 %	4000
	DME	2.1 %	93.7 %	4.2 %	4000
	NORMAL	0.5 %	3.8 %	95.8 %	4000
	Σ	4017	3967	4016	12000

Figure 6. Confusion matrix of neural network

Confusion Matrix

Confusion matrix for kNN (showing number of instances)

		Predicted CNV	DME	NORMAL	Σ
Actual	CNV	3784	110	106	4000
	DME	194	3199	607	4000
	NORMAL	31	140	3829	4000
	Σ	4009	3449	4542	12000

Confusion Matrix

Confusion matrix for kNN (showing proportion of actual)

		Predicted CNV	DME	NORMAL	Σ
Actual	CNV	94.6 %	2.8 %	2.6 %	4000
	DME	4.8 %	80.0 %	15.2 %	4000
	NORMAL	0.8 %	3.5 %	95.7 %	4000
	Σ	4009	3449	4542	12000

Figure 7. Confusion matrix of KNN

Confusion Matrix

Confusion matrix for Logistic Regression (showing number of instances)

		Predicted CNV	DME	NORMAL	Σ
Actual	CNV	3897	88	15	4000
	DME	89	3706	205	4000
	NORMAL	18	181	3801	4000
	Σ	4004	3975	4021	12000

Confusion Matrix

Confusion matrix for Logistic Regression (showing proportion of actual)

		Predicted CNV	DME	NORMAL	Σ
Actual	CNV	97.4 %	2.2 %	0.4 %	4000
	DME	2.2 %	92.7 %	5.1 %	4000
	NORMAL	0.5 %	4.5 %	95.0 %	4000
	Σ	4004	3975	4021	12000

Figure 8. Confusion matrix of LR

Confusion Matrix

Confusion matrix for Stack (showing number of instances)

		Predicted CNV	DME	NORMAL	Σ
Actual	CNV	3923	58	19	4000
	DME	70	3771	159	4000
	NORMAL	16	144	3840	4000
	Σ	4009	3973	4018	12000

Confusion Matrix

Confusion matrix for Stack (showing proportion of actual)

		Predicted CNV	DME	NORMAL	Σ
Actual	CNV	98.1 %	1.4 %	0.5 %	4000
	DME	1.8 %	94.3 %	4.0 %	4000
	NORMAL	0.4 %	3.6 %	96.0 %	4000
	Σ	4009	3973	4018	12000

Figure 9. Confusion matrix of stack

Following testing and training in this study, the system was used to predict whether the eyes were healthy or not. Then, importing the data as an image and applying models (ANN, KNN, LR, stack) detected two forms of eye illness (CNV, DME). The new picture was imported, analysed using the image embedding widget, and the eye state was predicted with the help of the prediction widget. As shown in Tables 1 and 2 belongs to case 1 and 2, respectively. Figure 10 shows the total results comparation for the three model through four algorithms.

Table 1. Prediction for data for case1

No.	Neural network	KNN	LR	Image name
1	CNV	CNV	CNV	CNV-53018-1
2	CNV	CNV	CNV	CNV-53018-2
3	normal	normal	CNV	CNV-81630-1
4	CNV	normal	CNV	CNV-8630-2
5	DME	normal	CNV	CNV-8630-3
6	DME	DME	DME	DME-30521-13
7	DME	DME	DME	DME-37503-1
8	DME	DME	DME	DME-57603-1
9	DME	DME	DME	DME-70266-1
10	DME	DME	DME	DME-70266-2
11	Normal	Normal	Normal	Normal-1249-1
12	Normal	Normal	Normal	Normal-1249-2
13	Normal	Normal	Normal	Normal-1249-3
14	Normal	Normal	Normal	Normal-1249-4
15	Normal	Normal	Normal	Normal-1249-5
16	Normal	Normal	Normal	Normal-1529-1
17	Normal	Normal	Normal	Normal-1530-1
18	Normal	Normal	Normal	Normal-3335-1
19	Normal	Normal	Normal	Normal-3335-2
20	Normal	Normal	Normal	Normal-3335-3
21	Normal	Normal	Normal	Normal-3363-1
22	Normal	Normal	Normal	Normal-3673-1
23	Normal	Normal	Normal	Normal-3781-1
24	Normal	Normal	Normal	Normal-4805-1
25	Normal	Normal	Normal	Normal-6047-1
26	Normal	Normal	Normal	Normal-9251-1

Table 2. Prediction for data for case 2

No.	LR (1)	KNN	Stack	Neural network	Image name
1	Normal	Normal	Normal	Normal	Normal-9251-1
2	Normal	Normal	Normal	Normal	Normal-6047-1
3	Normal	Normal	Normal	Normal	Normal-4805-1
4	Normal	Normal	Normal	Normal	Normal-3781-1
5	Normal	Normal	Normal	Normal	Normal-3673-1
6	Normal	Normal	Normal	Normal	Normal-3363-1
7	Normal	Normal	Normal	Normal	Normal3335-1
8	Normal	Normal	Normal	Normal	Normal-3335-2
9	Normal	Normal	Normal	Normal	Normal-3335-3
10	Normal	Normal	Normal	Normal	Normal-1530
11	Normal	Normal	Normal	Normal	Normal-1520
12	Normal	Normal	Normal	Normal	Normal-1249-1
13	Normal	Normal	Normal	Normal	Normal-1249-2
14	Normal	Normal	Normal	Normal	Normal-1249-3
15	Normal	Normal	Normal	Normal	Normal-1249-4
16	Normal	Normal	Normal	Normal	Normal-1249-5
17	DEM	DEM	DEM	DEM	DEM-70266-2
18	DEM	DEM	DEM	DEM	DEM-70266-1
19	DEM	DEM	DEM	DEM	DEM-57603-1
20	DEM	DEM	DEM	DEM	DEM-37503-1
21	DEM	DEM	DEM	DEM	DEM-30521-13
22	CNV	Normal	DEM	DEM	CNV-81630-1
23	CNV	Normal	CNV	CNV	CNV-81630-2
24	CNV	Normal	Normal	Normal	CNV-81630-1
25	CNV	CNV	CNV	CNV	CNV-53018-2
26	CNV	CNV	CNV	CNV	CNV-53081-1

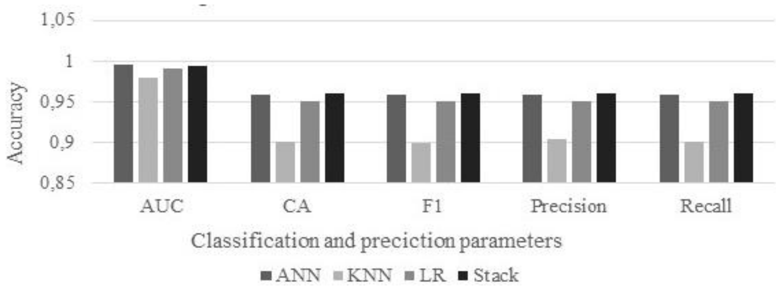

Figure 10. Comparison between the fourth proposed models

7. CONCLUSION

Using picture datasets from Kaggle, this research examines the potential of the orange data mining tool for automated image classification for three sets (CNV, DME), sick eye, and healthy eye. The KNN, ANN, and LR models were implemented in the first scenario, and they were trained and evaluated depending on the features that were collected from the photos. An orange tool's SqueezeNet-based image-embedded model was first used for the feature extraction procedure. Based on our research, we conclude that orange data mining tool is one of the most user-friendly and practical options for processing and analysing large datasets. Following this, the effectiveness of each classifier was evaluated using a confusion matrix and some estimation indices including AUC, classification accuracy (CA), F1 score, precision, and recall. The result of the numerical output demonstrates that the classifier depending on an ANN performs better than its competitors with regard to accuracy (0.958). The second case combined two models (KNN, ANN) and inserted the results we obtained from the two models into the third model (LR) by stacking the widget with an accuracy (0.961). This is higher accuracy than the first case, as well as we entered new data that the system was not trained to predict, and it made a very good prediction. If verified by further testing, this application can be used to screen diseases with distinctive visual features in clinical practice. In such situations, the clinician can use a picture in an online database to automatically evaluate and compare existing samples. This method will potentially increase the objectivity of the results and allow less-experienced clinicians more confidence as the system shows them the results compared to a wider selection of verified and documented cases.

REFERENCES

[1] S. Shurrab and R. Duwairi, “Self-supervised learning methods and applications in medical imaging analysis: a survey,” *PeerJ Computer Science*, vol. 8, p. e1045, Jul. 2022, doi: 10.7717/PEERJ-CS.1045.

[2] G. Haskins, U. Kruger, and P. Yan, “Deep learning in medical image registration: a survey,” *Machine Vision and Applications*, vol. 31, no. 1, Jan. 2020, doi: 10.1007/s00138-020-01060-x.

[3] R. S. Akinbo and O. A. Daramola, “Ensemble machine learning algorithms for prediction and classification of medical images,” in *Artificial Intelligence*, IntechOpen, 2021.

[4] H. A. Marzog, H. J. Abd, and A. Yonis, "Noise Removal of ECG signal using Multi-Techniques," in *2022 IEEE Integrated STEM Education Conference (ISEC)*, 2022: IEEE, pp. 397-403, doi: 10.1109/ISEC54952.2022.10025094.

[5] M. J. Mohsin, H. A. Marzog, and M. A. Therib, “Enhancement throughput and increase security of image transmitted over wireless network using (DNC),” *IOP Conference Series: Materials Science and Engineering*, vol. 928, no. 2, p. 22078, Nov. 2020, doi: 10.1088/1757-899X/928/2/022078.

[6] S. Kurnaz and M. A. H. Aljabery, “Predict the type of hearing aid of audiology patients using data mining techniques,” *Journal of Information Science and Engineering*, vol. 36, no. 2, pp. 205–215, Jun. 2020, doi: 10.1145/3234698.3234755.

[7] Y. Bar, I. Diamant, L. Wolf, S. Lieberman, E. Konen, and H. Greenspan, “Chest pathology detection using deep learning with non-medical training,” in *Proceedings - International Symposium on Biomedical Imaging*, Apr. 2015, vol. 2015-July, pp. 294–297, doi: 10.1109/ISBI.2015.7163871.

[8] D. A. A. Sabri and M. J. Mohsin, “A new algorithm for a steganography system,” *Engineering And Technology Journal*, vol. 33, no. 8, pp. 1955–1970, Oct. 2015, doi: 10.30684/etj.2015.108835.

[9] J. F. Salmon, *Kanski’s clinical ophthalmology E-book: A systematic approach*. Elsevier Health Sciences, 2019.

[10] C. Y. Cheung, F. Tang, D. S. W. Ting, G. S. W. Tan, and T. Y. Wong, “Artificial intelligence in diabetic eye disease screening,” *Asia-Pacific Journal of Ophthalmology*, vol. 8, no. 2, pp. 158–164, 2019, doi: 10.22608/APO.201976.

[11] G. I. Sayed, M. M. Soliman, and A. E. Hassanien, “A novel melanoma prediction model for imbalanced data using optimized SqueezeNet by bald eagle search optimization,” *Computers in Biology and Medicine*, vol. 136, p. 104712, Sep. 2021, doi: 10.1016/j.compbiomed.2021.104712.

[12] C. Sitaula and M. B. Hossain, “Attention-based VGG-16 model for COVID-19 chest X-ray image classification,” *Applied Intelligence*, vol. 51, no. 5, pp. 2850–2863, Nov. 2021, doi: 10.1007/s10489-020-02055-x.

[13] T. Nazir *et al.*, “Detection of diabetic eye disease from retinal images using a deep learning based centernet model,” *Sensors*, vol. 21, no. 16, p. 5283, Aug. 2021, doi: 10.3390/s21165283.

[14] V. A. Kumar *et al.*, “Comparative study on the optimization and characterization of soybean aqueous extract based composite film using response surface methodology (RSM) and artificial neural network (ANN),” *Food Packaging and Shelf Life*, vol. 31, p. 100778, Mar. 2022, doi: 10.1016/j.fpsl.2021.100778.

[15] A. N. Hassan, M. J. Mohsin, and A. H. K. Khwayyir, "Discrimination of ECG signal based on S-interpolation and quantum neural network," *Annals of Tropical Medicine and Public Health*, vol. 23, no. 10, 2020, doi: 10.36295/ASRO.2020.231039.
[16] S. Mohapatra and T. Swarnkar, "Comparative study of different orange data mining tool-based AI techniques in image classification," in *Lecture Notes in Networks and Systems*, vol. 202 LNNS, Springer Singapore, 2021, pp. 611–620.
[17] A. T. Hoang *et al.*, "A review on application of artificial neural network (ANN) for performance and emission characteristics of diesel engine fueled with biodiesel-based fuels," *Sustainable Energy Technologies and Assessments*, vol. 47, p. 101416, Oct. 2021, doi: 10.1016/j.seta.2021.101416.
[18] R. J. Huang, N. S.-E. Kwon, Y. Tomizawa, A. Y. Choi, T. Hernandez-Boussard, and J. H. Hwang, "A comparison of logistic regression against machine learning algorithms for gastric cancer risk prediction within real-world clinical data streams," *JCO Clinical Cancer Informatics*, no. 6, Jun. 2022, doi: 10.1200/cci.22.00039.
[19] H. A. Marzog, M. J. Mohsin, and M. A. Therib, "Chaotic systems with pseudorandom number generate to protect the transmitted data of wireless network," *Indonesian Journal of Electrical Engineering and Computer Science (IJEECS)*, vol. 21, no. 3, pp. 1602–1610, Mar. 2021, doi: 10.11591/ijeecs.v21.i3.pp1602-1610.
[20] E. Watanabe *et al.*, "Comparison among random forest, logistic regression, and existing clinical risk scores for predicting outcomes in patients with atrial fibrillation: A report from the J-RHYTHM registry," *Clinical Cardiology*, vol. 44, no. 9, pp. 1305–1315, Jul. 2021, doi: 10.1002/clc.23688.
[21] N. Hidayati and A. Hermawan, "K-nearest neighbor (K-NN) algorithm with euclidean and Manhattan in classification of student graduation," *Journal of Engineering and Applied Technology*, vol. 2, no. 2, Aug. 2021, doi: 10.21831/jeatech.v2i2.42777.
[22] S. Uddin, I. Haque, H. Lu, M. A. Moni, and E. Gide, "Comparative performance analysis of K-nearest neighbour (KNN) algorithm and its different variants for disease prediction," *Scientific Reports*, vol. 12, no. 1, Apr. 2022, doi: 10.1038/s41598-022-10358-x.
[23] H. A. Marzog and H. J. Abd, "ECG-signal classification using efficient machine learning approach," *In 2022 International Congress on Human-Computer Interaction, Optimization and Robotic Applications (HORA)*, Jun. 2022, doi: 10.1109/HORA55278.2022.9800092.
[24] Mohebbanaaz, L. V. R. Kumari, and Y. P. Sai, "Classification of arrhythmia beats using optimized K-nearest neighbor classifier," in *Lecture Notes in Networks and Systems*, vol. 185 LNNS, Springer Singapore, 2021, pp. 349–359.
[25] M. J. Mohsin, W. K. Saad, B. J. Hamza, and W. A. Jabbar, "Performance analysis of image transmission with various channel conditions/modulation techniques," *TELKOMNIKA (Telecommunication Computing Electronics and Control)*, vol. 18, no. 3, pp. 1158–1168, Jun. 2020, doi: 10.12928/TELKOMNIKA.v18i3.14172.

BIOGRAPHIES OF AUTHORS

Thanaa Hasan Yousif assistant Lecturer at Communication Techniques Engineering Department, Engineering Technical College-Najaf, Al-Furat Al-Awsat Technical University. She received Bachelor's and Master's degrees in Communication Techniques from Engineering Technical College-Najaf, Al-Furat Al-Awsat Technical University, Iraq in 2004 and 2020, respectively. Her current research interests include artificial intelligenceand machine learning. She can be contacted at email: thanaa.yousif.chm@atu.edu.iq.

Nahla Ali Tomah assistant Lecturer at Communication Techniques Engineering Department, Engineering Technical College-Najaf, Al-Furat Al-Awsat Technical University. She received Bachelor's College of Science, University of Kufa and Master's degrees in College of Education for Girls, University of Kufa, Iraq in 2002 and 2020, respectively. Her current research interests include artificial intelligenceand machine learning. She can be contacted at email: nahla.ali@atu.edu.iq.

Marwa Jaleel Mohsin she has been awarded a Ph.D. digree in communication and electronic engineering from university of Babylon/electrical engineering department, received master's degree in communication engineering from University of Technology/Electrical Engineering Department-Baghdad in 2015. She is currently an instructor in the engineering technical college of Najaf, Al-Furat Al-Awsat Technical University from 2007, her reserch interest include image processing, digital signal processing, digital communication, and optical wireless communication. She can be contacted at email: marwa.jaleel@atu.edu.iq.